Journal of the European Ceramic Society 19 (1999) 2465–2474

PII: S0955-2219(99)00122-3
0955-2219/99/$ - see front matter

Reaction-based Processing of Textured Alumina by Templated Grain Growth

Ender Suvaci, Matthew M. Seabaugh and Gary L. Messing*

Materials Research Laboratory, Department of Materials Science and Engineering,
The Pennsylvania State University, University Park, PA 16802, USA

Abstract

Highly textured, dense alumina ceramics were fabricated by a new processing route which utilizes a mixture of Al metal powder, alumina powder, alumina platelet (template) particles and a liquid phase former. The process involves dry forming the powder mixture (e.g. uniaxial pressing, and roll compaction) to align the plate-like template particles. The addition of a calcium aluminosilicate glass reduces constrained densification by the template particles and allows attainment of high density at ~1450°C. The degree of orientation (i.e. **r** *is 1 for a random sample and 0 for a perfectly textured material) and volume fraction of textured material,* ***f****, were measured by X-ray-based rocking curve technique and SEM-based stereological analysis, respectively. It has been shown that texture quality (the r parameter) is controlled by initial strain during forming, sintering time and temperature. In addition, alumina ceramics with the volume fraction of textured material ranging from 1 to ~100% can be obtained.*

Keywords: platelet templates, texturing, grain growth, microstructure-final, Al_2O_3.

1 Introduction

The physical properties of ceramics and ceramic matrix composites can be tailored by controlling microstructure. The goal of most processing studies has been the attainment of micrometer scale, equiaxed grains. Textured ceramics are interesting because they allow access to anisotropic properties which are similar to single crystal values. Many texture studies report the use of hot pressing and sinter forging to densify oriented anisometric particles such as fibers, whiskers and platelets.[1–4] These approaches are far too expensive to be commercially viable. A low cost and general approach for producing textured ceramics is templated grain growth.[5] Templated grain growth (TGG) is a technique for developing crystallographic texture in ceramic bodies via the grain growth of aligned anisometric particles in a dense and fine grain size matrix. With only 5% template particles nearly fully textured ceramics can be produced.[5] Initial studies of TGG concluded that the alignment of the template particles during forming, a fine-grain size, and a dense matrix are critical requirements for TGG.[5–9] Templates can be oriented by a variety of techniques, including tape casting, slip casting, centrifugal casting, and extrusion. In initial studies, dry forming techniques have not been preferred because the orientation is difficult to induce during pressing. Therefore, most TGG studies have relied on the use of colloidal processing.[5–11]

Textured α-Al_2O_3-based ceramics have been fabricated by a variety of techniques including hot pressing, sinter forging and tape casting.[4,12,13] In 1995, Brandon *et al.* fabricated a composite consisting of oriented α-Al_2O_3 platelet particles and equiaxed α-Al_2O_3 grains.[13–15] They reported improved bend strength, thermal shock resistance and inhibited crack propagation perpendicular to the tabular α-Al_2O_3 grains. Seabaugh *et al.* investigated texture development by templated grain growth in a liquid-phase sintered alpha alumina system as a function of template and liquid phase content, sintering time and temperature.[5] Templates were aligned by tape casting. They reported that the addition of CaO and SiO_2 creates favorable kinetic conditions for anisotropic grain growth during sintering. They were able to fabricate nearly 100% oriented α-Al_2O_3. Recently, An *et al.* investigated the use of the reaction bonding of aluminum oxide (RBAO) process and water-based gel casting to obtain textured alumina platelet reinforced RBAO composites.[16] They also used tape casting to align template particles. The initial composition was 45 vol% Al, 35 vol% α-Al_2O_3 and 20 vol% ZrO_2. They claimed that samples sintered for 5 h at 1550°C were ~80% texture;

*To whom correspondence should be addressed. Fax: +1-814-865-2326; e-mail: messing@mrl.psu.edu

however, they did not report how they determined the textured fraction. They focused on the mechanical properties of the samples rather than microstructural development and texture analysis. The processing of textured ceramic components by approaches described in the literature are limited to high temperatures (>1500°C), and are colloidal-based processes. These constraints lead to part size limitations, and/or limited texture.

The RBAO process is one of a number of reaction-based processes that have been developed to produce metal oxide materials. The process involves the use of aluminum and alpha alumina mixtures to produce alpha alumina-based ceramics.[17] The use of ductile Al powder in the initial mixture yields attractive characteristics such as low net shrinkage, high green strength, ease of green machining, and polymer-free processing (i.e., environmentally benign).[17–19] Moreover, if anisotropic particles are added to the initial mixture, ductile Al may allow control of orientation during dry forming operations like roll compaction, uniaxial pressing and double action pressing. In addition, when Al is converted to alumina, it results in a fine-grained alumina matrix which should result in a high driving force for grain growth of the oriented particles. In this paper we demonstrate that reaction-based processing and TGG can be combined in a new relatively low cost dry powder process to obtain highly textured alumina ceramics. A key element is the use of a liquid phase to avoid constrained densification by the template particles and to accelerate their growth.

2 Experimental Procedure

2.1 Materials and processing

A powder mixture of attrition milled Al, α-Al_2O_3 ($\sim$0·2 μm diameter, AKP-50 Sumitomo Chemical Co.), a liquid phase former (i.e. calcium aluminosilicate or magnesium aluminosilicate) and isopropanol was ball milled for 5 h with high purity α-Al_2O_3 balls (99% α-Al_2O_3) of 4 mm diameter in a plastic bottle. For the initial mixture, fine Al flakes with a high specific surface area ($\sim$20 m^2/g) were prepared by attrition milling a gas atomized spherical Al powder (2–5 μm diameter, Valimet, Inc., Stockton CA) with first 5 mm yttria stabilized tetragonal zirconia (YTZ) balls for 12 h, and then 1 mm YTZ balls for 8 h at 600 rpm. Temperature was kept at $\sim$20°C by a water cooling system during the milling. The milled Al powder was dried in air at $\sim$80°C.

The calcium aluminosilicate (CAS) glass was prepared by melting a mixture of 42·4 wt% SiO_2, 20·0 wt% α-Al_2O_3 and 37·6 wt% CaO at 1600°C for 2 h and quenching it in cold water. The magnesium aluminosilicate (MAS) glass with a composition of 21·5 wt% MgO, 17·5 wt% α-Al_2O_3 and 61·0 wt% SiO_2 was also prepared by the same heat treatment. The transparent glasses were crushed in a mortar and reduced to 0·2–3 μm by ball milling for 24–48 h with 4 mm diameter high purity α-Al_2O_3 balls. The eutectic temperatures for the CAS and MAS glasses are $\sim$1265[20] and 1355°C,[21] respectively.

After ball milling, 5 vol% alpha alumina platelets (Elf-Atochem) of 15–25 μm diameter and 2·0 μm thickness were added to the slurry. The platelets for TGG were washed prior to mixing by adding 10 wt% templates to water with a pH of 1 adjusted with a 7 wt% nitric acid solution. After sonification the slurry was boiled for 1 h. The platelets were separated and washed three more times. The platelets and matrix materials were stirred for 24 h. The slurry was dried in an oven at $\sim$80°C for 24 h and sieved to $<$90 μm (-170 mesh).

The powder mixture was uniaxially pressed to obtain pellets of 1·2 cm diameter and 0·1–0·5 cm thickness. Unless otherwise noted, powders were pressed at 285 MPa. The corresponding compaction ratio (i.e. initial height of the powder compact divided by the final height of the powder compact) was 6·7. After pressing, pellets were oxidized in a box furnace by heating at 5°C min^{-1} from room temperature to 450°C, then at 1°C min^{-1} from 450 to 1070°C and 5 h dwell at 1070°C in air. After oxidation, samples were heated at 5°C min^{-1} to the sintering temperature and held for 2 h.

2.2 Characterization

The particle size distributions of the α-Al_2O_3 and glass powders were determined by sedimentation. The specific surface area of the milled Al powders was measured by BET. The densities of the pressed pellets and sintered samples were determined by the dimensional method, and Archimedes' technique, respectively. Weight changes of the pellets were monitored with a thermogravimetric analyzer (TGA) during the reaction bonding process. High temperature X-ray diffraction (XRD) using CuK_α radiation was used to detect phase changes as a function of temperature. A thermomechanical analyzer (TMA) was used to compare the sintering behavior of the powder mixtures with and without a liquid phase former. Scanning electron microscopy (SEM) was used to examine microstructural development after oxidation, sintering and grain growth.

For crystallographic texture analysis, a X-ray-based rocking curve technique was chosen due to the simplicity of data collection and analysis. The rocking curve method is described elsewhere.[22]

Rocking curve measurements were performed around the $(000\overline{1}2)$ peak (i.e. 2 theta: 90·7°) of alpha alumina with rocking range in α of -40 to $+40$ θ using a standard diffractometer. The data were corrected to eliminate defocusing and absorption effects by a computer program developed by Vaudin.[23] The March–Dollase function, eqn (1), was chosen to quantify the measured textured distributions from the rocking curve analysis.[24] $P(f, r, \alpha)$, the texture compensation factor, is given by

$$P(f, r, \alpha) = f(r^2 \cos^2 \alpha + \frac{\sin^2 \alpha}{r}) + (1 - f) \quad (1)$$

where α = the angle between the texture (orientation) axis and the scattering vector, r = the degree of orientation, and f = the volume fraction of oriented material. In March's original paper, the **r** parameter is defined as the ratio of final thickness to initial thickness for the compact of rigid discs.[25] It is also related to the width of the texture distribution. For platelets, a low **r** value indicates a narrow distribution of platelet normal orientations about the sample normal. For a random sample $r = 1$ and $r = 0$ for a perfectly textured sample of platelet grains. The texture quality was evaluated as a function of compaction ratio, sintering time and temperature.

For the morphological texture analysis, sintered samples were examined by SEM. Micrographs of thermally etched sample cross sections were analyzed using image analysis software.[26] The area of each anisotropic grain and the dimensions of the major and minor axes were measured, along with α, the angle between major axis and sample surface. These values were corrected using Fullman relationships and r values obtained from the rocking curve data.[27] Since the volume fraction of highly textured materials (i.e. >60 vol%) is overestimated by the rocking curve technique,[27] f values were also calculated by stereological analysis.

3 Process Control

3.1 The modified reaction-based processing of alumina

To prevent contamination from the milling media the gas atomized spherical Al powder was separately attrition milled from the α-Al_2O_3 powder. To improve the milling efficiency, the Al powder was first attrition milled with 5 mm diameter YTZ balls for 12 h and then milled with 1 mm YTZ balls for 8 h. The contamination from the milling media was $<0{\cdot}03$ wt% which is significantly less than when the Al and α-Al_2O_3 powders are attrition milled together.[28] The specific surface area of the milled Al powder was ~ 20 m^2/g. The milled Al particles were flaky and smeared; therefore, instead of particle size, the specific surface area of the milled powder was used to characterize the milled Al powder. Ball milling and subsequent stirring were used to mix the Al, α-Al_2O_3, glass and template powders. A flow chart of the process is given in Fig. 1.

The green densities of samples were $60{\cdot}0 \pm 1{\cdot}0$% TD after uniaxial pressing at 285 MPa. The samples were heated in air at 5°C min^{-1} from room temperature to 450°C, then at 1°C min^{-1} from 450 to 1070°C to oxidize the Al in the system. Figures 2 and 3 show the TGA data and the XRD pattern of the 5 vol% CAS and 5 vol% platelet containing sample. According to the TGA data, the oxidation of Al begins at about 450°C. Below 450°C, $\sim 2{\cdot}5$% weight loss was observed due to decomposition of aluminium hydroxide. The reaction products below 450°C are mainly amorphous alumina; therefore, only alpha alumina and aluminum peaks can be observed by XRD. Above 450°C, the oxidation

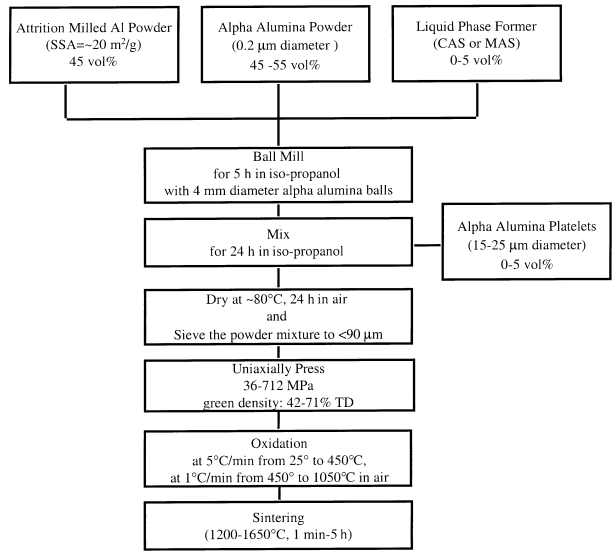

Fig. 1. Processing steps for the fabrication of textured reaction-based alumina ceramics by templated grain growth.

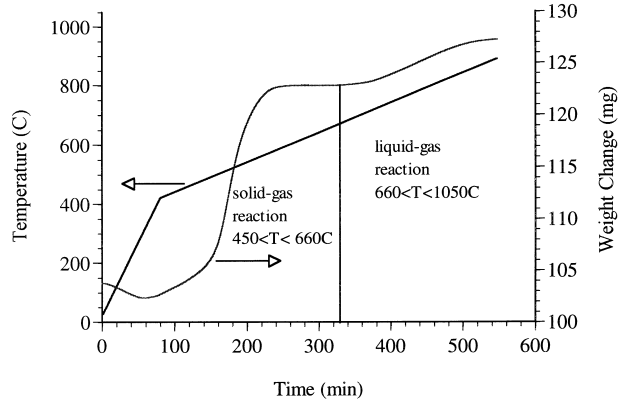

Fig. 2. Thermogravimetric analysis of 5 vol% CAS and 5 vol% platelet containing reaction-based alumina (initial sample weight: 104 mg).

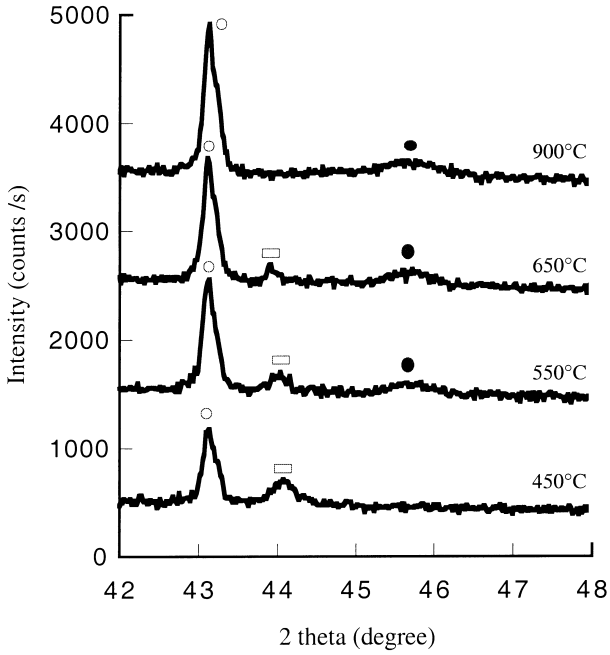

Fig. 3. XRD patterns of samples containing 5 vol% CAS and 5 vol% platelets as a function of temperature (□, aluminum; ○, alpha alumina; ●, gamma alumina).

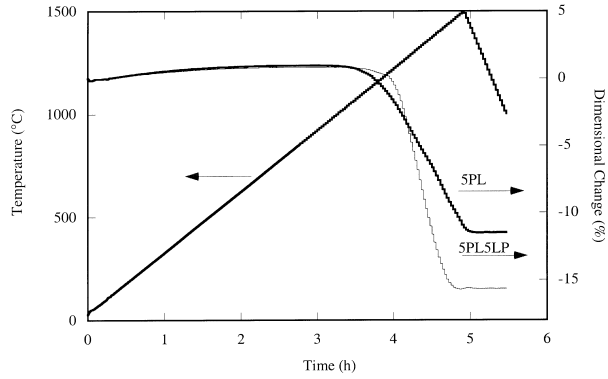

Fig. 4. Sintering behavior of 5 vol% platelet containing reaction-based alumina samples with (5PL5LP) and without calcium aluminosilicate doping (5PL).

rate increases until it reaches the maximum rate at ~550°C. Gamma-Al_2O_3 forms in this temperature range. This significant increase in oxidation rate can be caused by the formation of microcracks or channels (i.e. easy pathways for oxygen diffusion) in the amorphous alumina crust which surrounds the Al particles as a result of the crystallization of γ-Al_2O_3.[29] Between 550 and 660°C the reaction rate decreases because most of the Al is oxidized and diffusion of oxygen to the oxide-metal interface is inhibited by the oxide layer. For these oxidation conditions, ~82 wt% of the total oxidation occurred in the solid state for the samples containing 5 vol% CAS and 5 vol% platelets.

The melting of Al ($T_m = 660$°C) results in a 14 vol% increase in volume. Melting creates cracks in the alumina crust around the aluminum particles, and subsequently, more fresh Al is exposed. The oxidation of molten Al reaches a maximum rate at 850°C and oxidation is complete by ~900°C. Further heating of the samples results in the γ to α-Al_2O_3 transformation which is complete by ~1150°C.[30]

3.2 Liquid phase sintering of reaction-based alumina ceramics

To reduce the sintering temperature of the reaction-based alumina, liquid phase sintering was investigated. The CAS liquid promotes anisotropic grain growth whereas the MAS glass inhibits anisotropic grain growth.[31–34] A liquid phase reduces problems due to constrained sintering by large template particles. The effect of liquid phase former on shrinkage was measured by TMA by heating the completely oxidized samples at 5°C min^{-1} to 1500°C. In Fig. 4 the TMA data shows that the liquid phase containing sample, 5PL5LP (5 vol% platelets and 5 vol% CAS), fully densifies at ~1450°C whereas the undoped sample 5PL (0 vol% CAS and 5 vol% platelets) was ~84% dense at 1500°C.

Figure 5(a)–(c) shows micrographs of undoped, 5 vol% CAS-doped and 5 vol% MAS-doped reaction-based alumina ceramics, respectively, which were sintered at 1600°C for 2 h. The undoped sample consists of relatively equiaxed grains with an average size of 2·5 μm. On the other hand, the CAS and MAS-doped samples exhibit an average grain size of 5·0 and 4·5 μm, respectively. In addition, the undoped sample is ~95% dense, and the CAS and MAS-doped samples are ~97% dense, based on SEM studies. This higher density in the doped samples can be attributed to elimination of large defects [arrowed in Fig. 5(a)] during liquid phase sintering.

3.3 Template grain growth

The effect of template particles on microstructure was examined by adding 5 vol% alumina platelets to undoped and 5 vol% CAS-doped reaction-based alumina. The samples were sintered at 1600°C for 2 h. Figure 6(a) demonstrates that the final microstructure of the platelet containing, undoped sample consists of anisotropic grains with an average grain size of 25 μm and a thickness of ~2 μm distributed in a fine (~2 μm) matrix. The sample is ~92% dense and the degree of orientation of anisotropic grains is ~0·55. Figure 6(b) shows a micrograph of the sample containing 5 vol% CAS and 5 vol% platelets. The microstructure consists of faceted, anisotropic grains with an average particle size of 43 μm and a thickness of 7·8 μm distributed in a fine grain alpha alumina matrix of ~5 μm. The volume fraction of oriented grains is >80% and the degree of orientation, r, is 0·4.

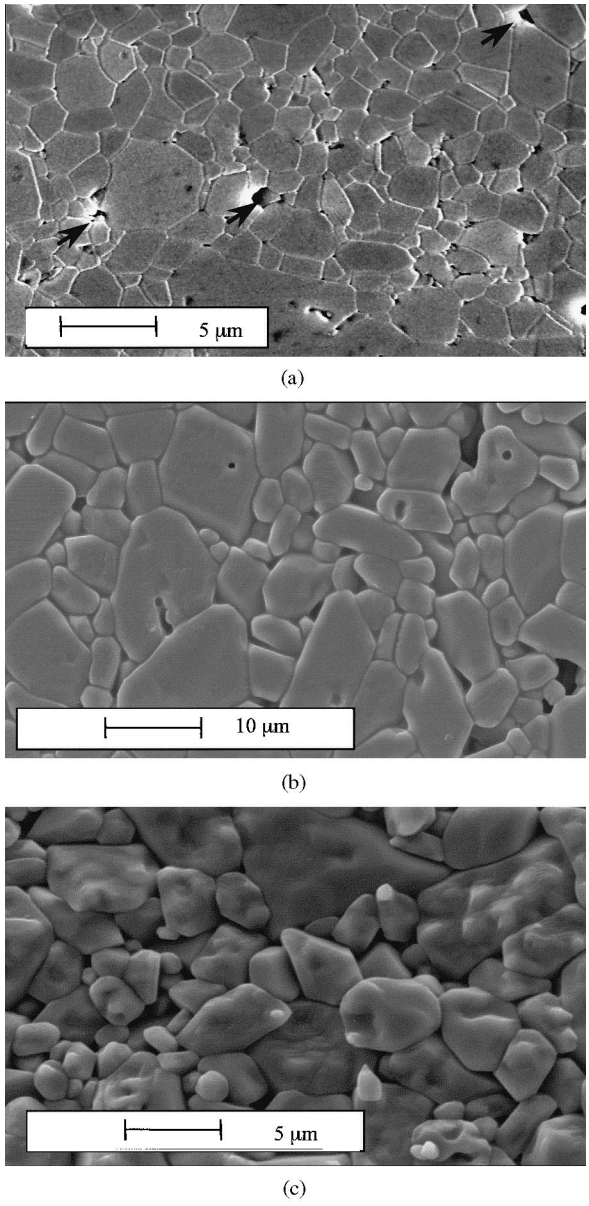

Fig. 5. SEM micrographs of (a) undoped, (b) CAS-doped and (c) MAS-doped reaction-based alumina; 1600°C, 2 h.

The poor grain growth and densification behavior of the undoped sample can be attributed to the gaps around the large anisotropic grains and thus, the template particles did not have intimate contact with the matrix during heating. It is likely that since the matrix grains are much finer than the platelets they densified away from the platelets. Moreover, the ~19% volume shrinkage during the gamma to alpha alumina transformation in the matrix may have caused the separation of platelets from the matrix grains. The CAS-doped samples do not exhibit this kind of separation or constrained densification of platelets. The platelets in the CAS-doped samples demonstrate extensive grain growth and a microstructure that exhibits a high volume fraction of faceted grains. This high degree of texture indicates that the CAS liquid promotes grain growth and large anisotropic grains grow by an Ostwald ripening type process.

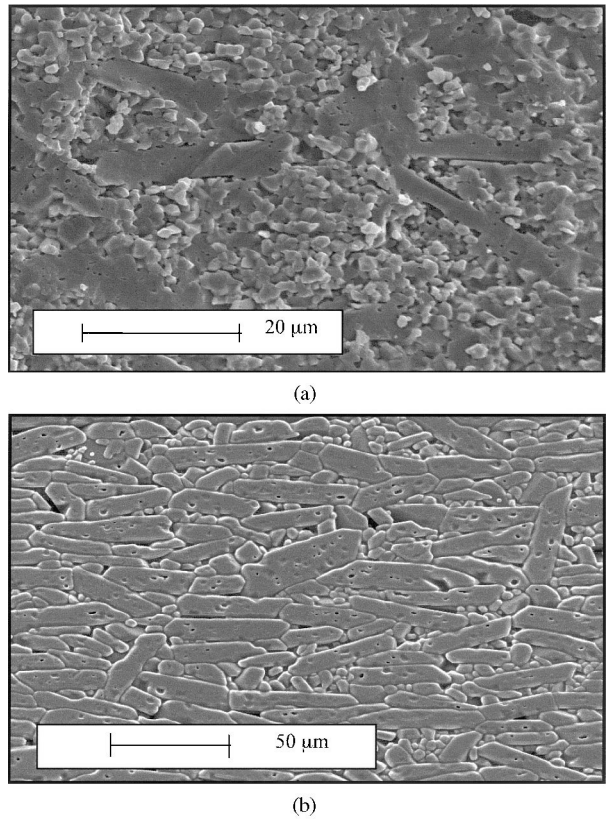

Fig. 6. SEM micrographs of (a) 5 vol% platelet and 0 vol% CAS containing sample (5PL), and (b) 5 vol% platelet and 5 vol% CAS containing sample (5PL5LP); 1600°C, 2 h.

These observations are similar to those of Seabaugh et al for CAS-doped boehmite-derived alpha alumina system.[5] The comparison in Fig. 6 also reveals that alignment of anisotropic particles (i.e. degree of orientation) in CAS-doped sample (i.e. $r = 0{\cdot}4$) is much better than that in the sample without CAS (i.e. $r = 0{\cdot}55$). This result suggests that the liquid phase helps to align template particles by a rearrangement process and thus improves texture quality.

4 Texture Development

4.1 Compaction ratio

Powders were pressed over a range of compaction ratios to determine how it affected texture development. Figure 7 demonstrates the effect of compaction pressure on the compaction ratio and the green density for 5 vol% CAS and 5 vol% platelet containing samples. The compaction ratio ranged from 3·8 to 8·1 and the green density ranged from 41 to 71%. Higher compaction ratios result in higher green densities and subsequently better packing of the particles. The high densities are a direct consequence of the presence of the ductile Al.

Micrographs of sintered samples which were formed at compaction ratios of 3·8, 5·6, 7·7 and 8·1 and then sintered at 1600°C for 2 h, are shown in

Fig. 8(a)–(d), respectively. As the compaction ratio increases, the volume fraction of oriented material increases. For example, while the textured fraction for the sample with a 3·8 compaction ratio is ~55%, it is >90% for the sample with a compaction ratio of 8·1. The higher green densities result in higher sintered densities. For instance, although the sample with a 3·8 compaction ratio is 94% dense, the density of the sample with a compaction ratio of 8·1 is ~98%. Moreover, the amount of porosity within grains decreases with increasing compaction ratio. This observation suggests that higher green densities allow attainment of full densification before the start of grain growth and subsequently, less amount of porosity will be available to be swept into grains during grain growth. Thus, the high green density obtained at high strain favors both template orientation as well as the elimination of pores in the green compact which can become trapped in grains during growth.

Figure 9 shows how the degree of orientation of the sintered samples depends on the compaction ratio. For compaction ratios from 3·8 to 5·6, r decreases slowly as the compaction ratio increases. Between 5·6 and 7·1, the green density exceeds 64% and r significantly decreases with increasing

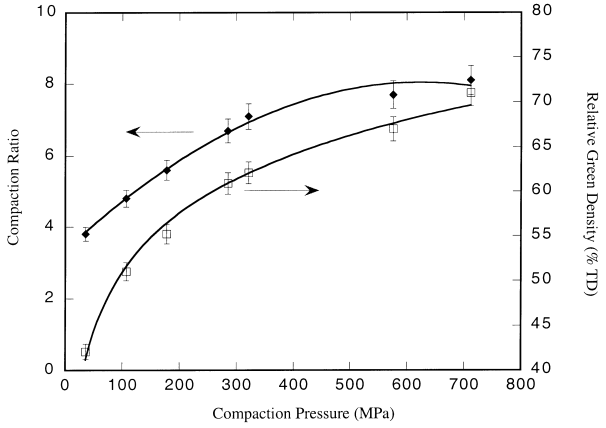

Fig. 7. The effect of compaction pressure on compaction ratio and green density (5PL5LP).

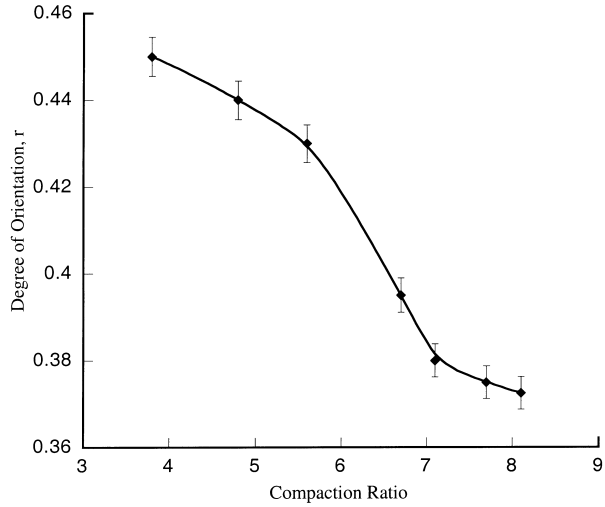

Fig. 9. The effect of compaction ratio on the degree of orientation of the 5PL5LP samples when heated at 1600°C for 2 h.

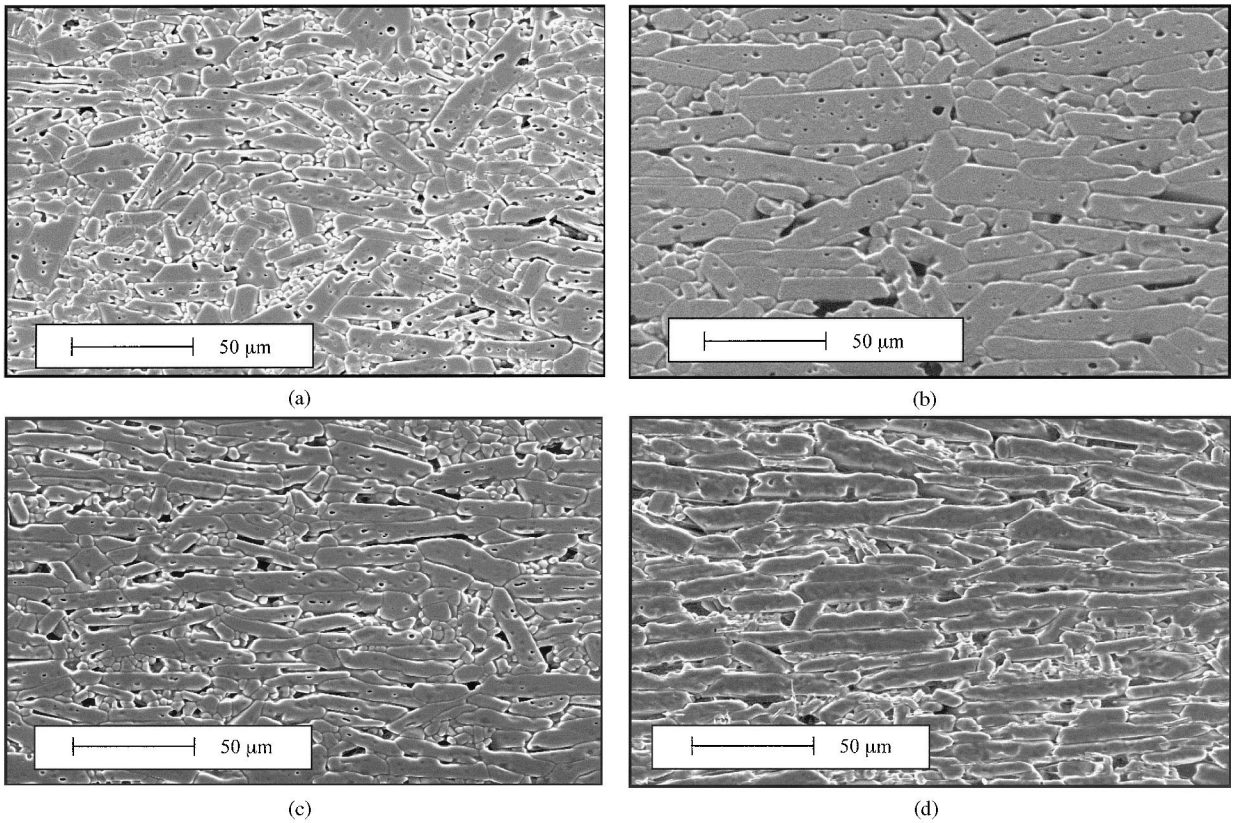

Fig. 8. SEM micrographs of 5PL5LP samples which exhibited (a) 3·8, (b) 5·6, (c) 7·7 and (d) 8·1 compaction ratios during forming; 1600°C, 2 h.

compaction ratio. Above 7·1, r changes very slowly with the compaction ratio. These results show that the presence of Al in the initial mixture allows the attainment of higher compaction ratios and thus better control of texture development. For example, high degrees of texture were obtained at compaction ratios $>6{\cdot}5$ for green densities $\geq$60% TD. Such densities would be difficult to achieve by dry pressing unless a ductile metal is present.

4.2 Sintering temperature

Figure 10(a)–(d) shows microstructures of 5 vol% CAS and 5 vol% platelet containing samples which were formed at a compaction ratio of 6·7 and sintered at 1070, 1400, 1500 and 1650°C. Figure 10(a) shows the microstructure of the sample after the oxidation stage but below the eutectic temperature of the glass phase ($T_{E,CAS}$:$\sim$ 1265°C) and below the γ to α alumina transformation temperature. Although there are a few misoriented templates, most of templates are aligned perpendicular to the pressing direction and the initial microstructure consists of platelets with an average size of 20 by 2·0 μm distributed in a very fine (0·02–0·2 μm) matrix of gamma and alpha alumina. Since densification has not started yet, the densities of samples are between 55 and 60% TD.

When sintered at 1400°C for 2 h, the >90% dense sample consists of α alumina. At this point the platelets grow to an average size of 25·3 by 2·5 μm with an aspect ratio of 12. The degree of orientation is 0·62 and the volume fraction of oriented materials is $\sim$12 vol%. When the samples are sintered at 1500°C for 2 h [Fig. 10(c)], there is rapid densification to 95% TD and grain growth due to the higher temperature and development of 6·5 vol% liquid. The samples consist of platelets with an average size of 41·2 by 5·6 μm and an average aspect ratio of 7·5. The template grains are well-oriented, but some misorientation from the initial microstructure is still present. The degree of orientation is 0·38 and the volume fraction of oriented materials is $\sim$40 vol%. At 1650°C, there is 7·9 vol% liquid and after 2 h sintering, the samples are $\geq$95% dense. The microstructure consists of >90% oriented alpha alumina with an average grain size of 50 by 10 μm and a smaller aspect ratio of 5 compared to the 1500°C. The degree of orientation is 0·4.

Examination of the temperature dependence of the degree of orientation demonstrates that r decreases from 0·62 to 0·38 between 1400 and 1500°C and remains essentially constant at 1650°C. The increased orientation between 1400 and 1500°C can be attributed to the increase in liquid phase content and a decrease in the viscosity of liquid phase. These factors are favorable for grain rearrangement and/or the interaction between anisotropic grains. As the temperature increases, the volume fraction of oriented materials increases

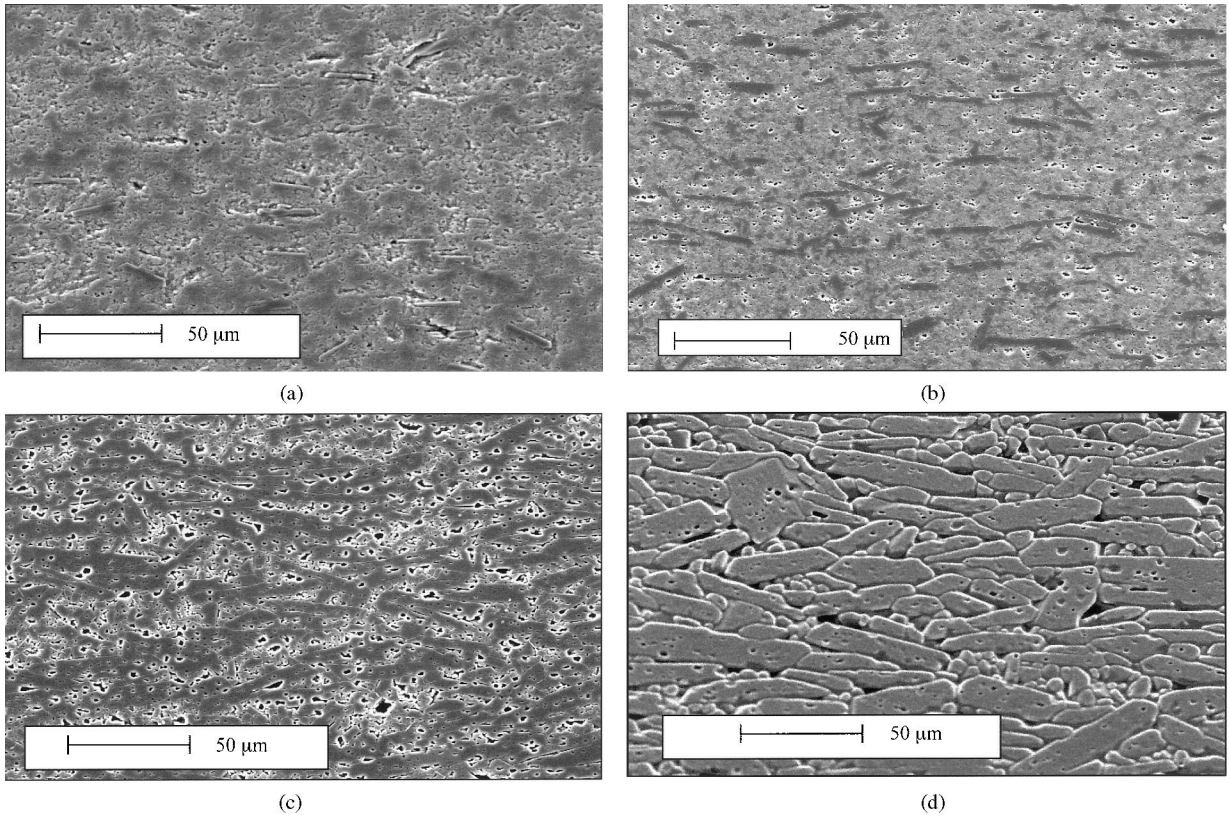

Fig. 10. Microstructure evolution of 5PL5LP samples, sintered at (a) 1070°C, 5 h; (b) 1400°C; (c) 1500°C; (d) 1650°C for 2 h (compaction ratio: 6·7).

from 12 to 40% between 1400 and 1500°C and to >90% at 1650°C. At 1400°C, the aspect ratio of anisotropic grains is about the same as the aspect ratio of the initial platelets (i.e. ~13). Between 1400 and 1500°C, the aspect ratio decreases from 12 to 7·5. This decrease in the aspect ratio is attributed to impingement of the anisotropic grains in the length direction and subsequent growth in the thickness due to the presence of smaller alpha alumina grains. The decrease in aspect ratio corresponds to when the textured fraction is 40% which is near the percolation threshold of 0·44 for discs in two dimensions.[35] The aspect ratio further decreases to 5 after sintering at 1650°C for 2 h. Interestingly, as the volume fraction of the textured material increases from 40 to 90% most of the template growth occurs by grain thickening.

4.3 Sintering time

To evaluate the influence of sintering time on texture development, CAS-doped samples with 5 vol% platelets were formed at a compaction ratio of 6·7 and sintered at 1600°C for 1–300 min. Approximately ~7·3 vol% liquid develops at this temperature. After 1 min, the ~95% dense microstructure consists of about 54 vol% anisotropic grains with an average grain size of 40·2 by 6·0 μm and alpha alumina matrix grains of ~4·5 μm [Fig. 11(a)]. The degree of orientation is 0·58 and there are a few misoriented grains in the microstructure. The microstructure shows that the large grains have impinged with each other. Consequently, the aspect ratio is 6·6. After 300 min sintering, the microstructure exhibits faceted and well oriented (i.e. $r = 0{\cdot}4$) anisotropic grains with an average grain size of 49·2 by 8·9 μm. The volume fraction of oriented grains is ~90 vol%. The remaining matrix grains exhibit an average grain size of ~7 μm which limits the rate of grain growth.

Figure 12 shows how the textured fraction and aspect ratio change with sintering time at 1600°C. The initial grains grow very rapidly upon heating with the volume fraction of oriented material increasing to 54%. When the sample is heated for 300 min ~90% of the sample consists of oriented grains. The aspect ratio of platelets decreases with increasing time from 6·6 in Fig. 11(a) to 5·6 in Fig. 11(b). In addition, the number of grains decreases with increasing sintering time. The degree of orientation increases as r decreases from 0·58 to 0·4 between 1 and 300 min.

5 Discussion

This study shows that highly textured (>90%), dense (≥95% TD) alumina ceramics can be fabricated by a new, relatively low cost processing route which uses a mixture of Al metal powder, alumina powder, alumina platelet (template) particles and a liquid phase former.[36] The process involves the use of dry forming techniques such as pressing and roll compaction to align template particles. Unlike initial texture forming processes such as gel casting,[11–14] tape casting[5,11–14] this process does not require any polymer additives and other processing difficulties such as sol-gel, lamination and binder burn out. In addition, the use of metal forming techniques allows fabrication of large parts which is not easy with colloidal-based processes.

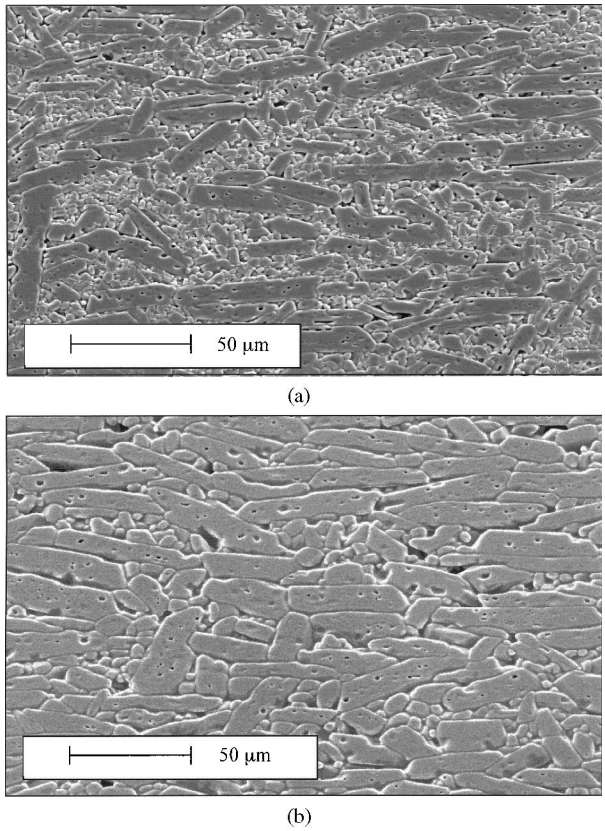

Fig. 11. SEM micrographs of 5PL5LP samples (compaction ratio: 6·7), sintered at 1600°C for (a) 1 and (b) 300 min.

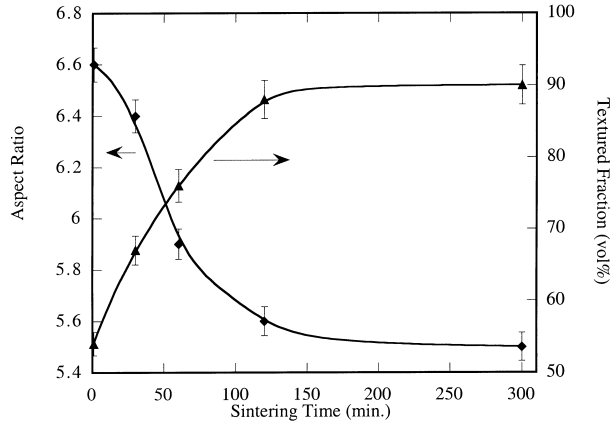

Fig. 12. The effect of sintering time on aspect ratio of anisotropic grains and volume fraction of 5PL5LP at 1600°C.

Furthermore, the low net shrinkage of the RBAO process enables the fabrication of large textured parts.

Although An *et al.*[14] did not report how much zirconia was added from the milling media to the initial RBAO mixture during the attrition milling, Holz *et al.*[17] reported an uncontrolled zirconia contamination from the milling media between 3 and 5 wt% under similar milling conditions. In this study, separate milling of Al powders allowed controlled and relatively clean (i.e. zirconia free) processing of reaction-based alumina ceramics. The degree of orientation of the final microstructure can be controlled by the consolidation process due to ductility of the Al metal powder. High degrees of texture were obtained at compaction ratios $\geq$6·5 and a green density of $\geq$60% TD which would be difficult to achieve without Al. In the initial RBAO studies,[15–17] the authors claim that to improve the oxidation and densification, yttria and zirconia were added to the initial mixture. In this study, the addition of a liquid phase former reduces the sintering temperature of reaction bonded alumina ceramics to temperatures as low as ~1450°C. Moreover, due to the use of a liquid phase and the increased driving force for TGG due to very fine matrix grain size resulting from the oxidized Al powder, very large final grain sizes (up to 100 μm) can be achieved [Fig. 8(d)].

Templates dominated the grain growth and controlled texture development in CAS containing systems as observed by Seabaugh *et al.*[5] On the other hand, in systems with no CAS, separation between template particles and matrix grains was observed. Therefore, grain growth did not occur in these samples. Consequently, the presence of both CAS and template particles is critical for templated grain growth in reaction-based alumina systems.

6 Conclusions

Near fully textured, dense (95–98% TD) alumina ceramics were successfully fabricated by a new processing route which uses a mixture of Al metal powder, alumina powder, alumina platelet (template) particles and a liquid phase former. Unlike other texturing processes such as tape casting, gel casting and slip casting, this process uses dry forming techniques such as uniaxial pressing, forging and roll compaction to align template particles. The addition of a liquid phase former to the initial mixture allows sintering of reaction bonded alumina ceramics at low temperatures (~1450°C). In addition, the liquid phase former improved densification and grain growth. The degree of orientation (i.e. texture quality) can be controlled readily by the compaction ratio during the consolidation process. Sintering time and temperature control the volume fraction of oriented material and the degree of orientation.

Acknowledgements

The authors would like to thank Mr Herb McKinstry for performing the high temperature XRD operations. Dr Mark D. Vaudin, NIST, is thanked for providing the software for rocking curve texture analysis and useful suggestions. E.S. gratefully acknowledges the technical assistance of Bahar Suvaci during the stereological texture analysis. He also would like to thank the Turkish Ministry of National Education for the Overseas Scholarship.

References

1. Kimura, T., Yashimoto, T., Iida, N., Fujita, Y. and Yamaguchi, T., Mechanism of grain orientation during hot-pressing of bismuth titanate. *J. Am. Ceram. Soc.*, 1989, **72**, 85–89.
2. Takenaka, T. and Sakata, K., Grain orientation and electrical properties of hot-forged $Bi_4Ti_3O_{12}$ ceramics. *Jap. J. Appl. Phys.*, 1980, **19**, 31–39.
3. Igarashi, H., Matsunaga, Taniai, T. and Okazaki, K., Dielectric and piezoelectric properties of grain-oriented $PbBi_2Nb_2O_9$ ceramics. *Am. Ceram. Soc. Bull.*, 1978, **57**(9), 815–817.
4. Ma, Y. and Bowman, K. J., Texture in hot pressed or forged alumina. *J. Am. Ceram. Soc.*, 1991, **74**(11), 2941–2944.
5. Seabaugh, M. M., Kerscht, I. H. and Messing, G. L., Texture development by templated grain growth in liquid-phase sintered α-alumina. *J. Am. Ceram. Soc.*, 1997, **80**(5), 1181–1188.
6. Brahmaroutu, B., Messing, G. L., Trolier-McKinstry, S. and Selvaraj, U., Templated grain growth of textured Sr2Nb2O7. In *ISAF'96 Proceedings of the Tenth IEEE International Symposium on Applications of Ferroelectrics Volume II*, ed. B. M. Kulwicki, A. Amin and A. Safari. IEEE, Piscataway, NJ, 1996.
7. Seabaugh, M. M., Hong, S. H. and Messing, G. L., Processing of textured ceramics by templated grain growth. In *Ceramic Microstructure: Control at the Atomic Level*, ed. A. P. Tomsia and A. Glaeser. Plenum Press, New York, 1998, pp. 303–310.
8. Horn, J. A., Zhang, S. C., Selvaraj, U., Messing, G. L. and Trolier-McKinstry, S., Templated grain growth of textured bismuth titanate. *J. Am. Ceram. Soc.*, 1999, **82**(4), 921–926.
9. Hong, S. H. and Messing, G. L., Development of textured mullite by templated grain growth. *J. Am. Ceram. Soc.*, 1999, **82**(4), 867–872.
10. Sacks, M. D., Scheiffele, G. W. and Staab, G. A., Fabrication of textured silicon carbide via seeded anisotropic grain growth. *J. Am. Ceram. Soc.*, 1996, **79**(6), 1611–1616.
11. Hirao, K., Ohashi, M., Brito, M. and Kanzaki, S., Processing strategy for producing highly anisotropic silicon nitride. *J. Am. Ceram. Soc.*, 1995, **78**(6), 1687–1690.
12. Huber, J., Krahn, W., Ernst, J., Bocker, A. and Bunge, H. J., Texture formation in alumina. *Materials Science Forum*, 1994, **157–162**, 1411–1416.

13. Carisey, T., Laguier-Werth, A. and Brandon, D. G., Control of texture in Al_2O_3 by Gel-Casting. *J. Eur. Ceram. Soc.*, 1995, **15**, 1–8.
14. Carisey, T., Levin, I. and Brandon, D. G., Microstructure and mechanical properties of textured α-Al_2O_3. *J. Eur. Ceram. Soc.*, 1995, **15**, 283–289.
15. Brandon, D. G., Chen, D. and Chan, H., Control of texture in monolithic alumina. *Mater. Sci. Eng.*, 1995, **A195**, 189–196.
16. An, L., Wu, S., Chan, H. M., Harmer, M. P. and Brandon, D. G., Alumina platelet reinforced reaction bonded aluminum oxide composites: textured and random. *J. Mater. Res.*, 1997, **12**(12), 3300–3306.
17. Claussen, N., Le, T. and Wu, S., Low shrinkage reaction bonded alumina. *J. Eur. Ceram. Soc.*, 1989, **5**, 29–35.
18. Claussen, N., Wu, S. and Holz, D., Reaction bonding of aluminum oxide (RBAO) composites: processing, reaction mechanisms and properties. *J. Eur. Ceram. Soc.*, 1994, **14**, 97–109.
19. Holz, D., Wu, S., Scheppokat, S. and Claussen, N., Effect of processing parameters on phase and microstructure evolution in RBAO ceramics. *J. Am. Ceram. Soc.*, 1994, **77**(10), 2509–2517.
20. Osborn, E. F. and Muan, A., The System CaO–Al_2O_3–SiO_2. In Plate No 1 in Phase Equilibrium Diagrams of Oxide Systems. The American Ceramic Society, Columbus, Ohio, 1960, pp. 219–221.
21. Bergeron, C. G. and Risbud, S. H., Introduction to Phase Equilibria in Ceramics. The American Ceramic Society, Westerville, Ohio, 1984, pp. 114–116.
22. Vaudin, M. D., Ruprich, M. W., Jowett, M., Riley, Jr., G. N. and Bingert, J. F., A method for crystallographic texture investigation using standard X-ray equipment. Submitted for publication to *J. Mat. Res.*, 1998.
23. Texture, by Vaudin, M. D., National Institute of Standards and Technology, Gaithersburg, MD, USA available upon request.
24. Dollase, W. A., Correction of intensities for preferred orientation in powder diffractometry: application of the March model. *J. Appl. Cryst.*, 1986, **19**, 267–272.
25. March, A., Mathematische Theorie der Regelung nach der Korgestalt bei Affiner Deformation. *Z. Kristtallogr.*, 1932, **81**, 285–297.
26. NIH Image, v. 1.56 by Rasband, W., National Institutes of Health, USA.
27. Seabaugh, M. M., Texture development in liquid phase sintered alumina via anisotropic template growth. Ph.D. thesis, The Pennsylvania State University, 1998.
28. Derby, B., Reaction bonding of ceramics by gas–metal reactions. In *Ceramic Processing Science and Technology, Ceramic Transactions 51*, ed. H. Hausner, G. L. Messing and S. Hirano. The American Ceramic Society, Westerville, Ohio, 1995, pp. 217–224.
29. Wefers, K. and Misra, C., Oxides and Hydroxides of Aluminum. Alcoa Tech. Paper No. 19, Rev., Alcoa Labs, 1987.
30. Suvaci, E. and Messing, G. L., Processing parameter effects on the reaction bonding of aluminum oxide process. *J. Matl. Sci.*, 1999, **34**, in press.
31. Kaysser, W. A., Sprissler, M., Handwerker, C. A. and Blendell, J. E., Effect of a liquid phase on the morphology of grain growth in alumina. *J. Am. Ceram. Soc.*, 1987, **70**(5), 339–343.
32. Handwerker, C. A., Morris, P. A. and Coble, R. L., Effects of chemical inhomogeneities on grain growth and microstructure in Al_2O_3. *J. Am. Ceram. Soc.*, 1989, **72**(1), 130–136.
33. Song, H. and Coble, R. L., Origin and growth kinetics of platelike abnormal grains in liquid phase sintered alumina. *J. Am. Ceram. Soc.*, 1990, **73**(7), 2077–2085.
34. Song, H. and Coble, R. L., Morphology of platelike abnormal grains in liquid phase sintered alumina. *J. Am. Ceram. Soc.*, 1990, **73**(7), 2086–2090.
35. Holm, E. A. and Cima, M. J., Two-dimensional whisker percolation in ceramic matrix-ceramic whisker composites. *J. Am. Ceram. Soc.*, 1989, **72**(2), 303–305.
36. Messing, G. L. and Suvaci, E., US Patent Pending.